

The Mechanism of Reaction of Ferricyanide-Pretreated Mixed-Valence-State Membrane-Bound Cytochrome Oxidase with Oxygen at 173 K

By G. MARIUS CLORE* and EDWIN M. CHANCE

Department of Biochemistry, University College London, Gower Street, London WC1E 6BT, U.K.

(Received 19 December 1977)

1. The results of non-linear optimization studies on the mechanism of reaction of ferricyanide-pretreated mixed-valence-state cytochrome oxidase with O_2 at 173 K are presented. The analysis is carried out on data obtained by means of dual-wavelength multi-channel spectroscopy at four wavelength pairs (444–463 nm, 604–630 nm, 608–630 nm and 830–940 nm) and at two O_2 concentrations (360 μM and 520 μM). The only model that satisfies the triple requirement of a standard deviation within the standard error of the experimental data, a random distribution of residuals and good determination of the optimized parameters, is a three-intermediate sequential mechanism. 2. On the basis of the optimized values of the relative absorption coefficients of the intermediates at each wavelength obtained from the present paper together with data from optical wavelength scanning and e.p.r. spectroscopy obtained by low-temperature trapping studies, the possible valence states of the metal centres in each of the intermediates are discussed.

The minimal functioning unit of cytochrome oxidase (EC 1.9.3.1), the terminal complex of the mitochondrial respiratory chain, is thought to contain two haems, a and a_3 , and two copper atoms (Lemberg, 1969; Muijsers *et al.*, 1972; Caughey *et al.*, 1976). One copper atom, termed Cu_A , is detectable by e.p.r. spectroscopy (Aasa *et al.*, 1976) and thought to be magnetically isolated (Palmer *et al.*, 1976). The other copper atom, termed Cu_B , is undetectable by e.p.r. (Aasa *et al.*, 1976) and anti-ferromagnetically coupled to high-spin haem a_3^{3+} when in the cupric state (Palmer *et al.*, 1976; Thomson *et al.*, 1976, 1977; Falk *et al.*, 1977). [The notation used to designate the two copper atoms is that of Clore & Chance (1978) and Palmer *et al.* (1976), and will be used throughout the present paper.]

In the preceding paper (Clore & Chance, 1978) we analysed the kinetics of the reaction of fully reduced membrane-bound cytochrome oxidase with O_2 at 176 K by means of multi-channel dual-wavelength spectroscopy at three wavelength pairs, and non-linear stiff numerical integration and optimization techniques to evaluate quantitatively the experimental data. The only model that satisfied the triple requirement of a standard deviation within the standard error of the experimental data, good determination of the optimized parameters and a random distribution of residuals, was a three-species sequential mechanism. This established the presence of another

intermediate in the reaction of fully reduced membrane-bound cytochrome oxidase with O_2 at low temperatures that had not been identified by low-temperature trapping and wavelength-scanning optical spectroscopy (Chance *et al.*, 1975*b,c*).

The present study concerns the elucidation of the kinetics and chemistry of the reaction of ferricyanide-pretreated mixed-valence-state membrane-bound cytochrome oxidase with O_2 at 173 K by means of the techniques developed by Clore & Chance (1978). A combination of spectroscopic, e.p.r. and potentiometric studies (Mackay *et al.*, 1973; Lindsay & Wilson, 1974; Lindsay *et al.*, 1975; Wilson *et al.*, 1975; Chance *et al.*, 1978) have shown that pretreatment of the fully reduced membrane-bound cytochrome oxidase-CO complex with ferricyanide results in the oxidation of all components of the respiratory chain having midpoint potentials less than 300 mV. Only haem a_3 and Cu_B (midpoint redox potentials at pH 7.2 of 380 ± 10 mV and 340 ± 10 mV respectively) remain reduced, haem a and Cu_A being oxidized together with all the other components of the respiratory chain. This permits one to obtain further insight into the reaction of cytochrome oxidase with O_2 and the interactions of its four metal centres. Two spectroscopically distinct species, A_2 and C , have been identified by using the low-temperature trapping technique (Chance *et al.*, 1975*b,c*; Denis & Chance, 1977; Chance & Leigh, 1977). Compound A_2 had a 590 nm α -band with a shoulder at 600 nm and a trough at 612 nm, a 546 nm β -band and a negative 444 nm γ -band with a small

Abbreviation used: m.c.d., magnetic circular dichroism.

* To whom correspondence should be addressed.

423 nm peak. Compound C had identical features in the Soret region, a 547 nm β -band, and an intense absorption band in the α -region at 606–609 nm. Compound A₂ was recognized as functional by its conversion into compound C.

The experimental data for the present study were obtained by means of dual-wavelength multi-channel spectroscopy at four wavelength pairs (444–463 nm, 604–630 nm, 608–630 nm and 830–940 nm) and at two O₂ concentrations (360 μ M and 520 μ M).

Experimental

Biochemical methods

The preparation of the CO-inhibited fully reduced mitochondrial suspension is identical with that described (Clare & Chance, 1978) except that K₃FeCN₆ (at a final concentration of 5 mM) is added at 253 K and allowed to react for 1 min before the addition of the oxygenated ethylene glycol solution followed by rapid cooling to 195 K. Lanne *et al.* (1977) have tentatively suggested on the basis of optical and e.p.r. studies that ferricyanide slowly reacts at room temperature (298 K) with purified soluble cytochrome oxidase over a period of approximately 50 min to form a complex whose redox properties differ from those of the free soluble cytochrome oxidase. However, at the low temperatures used in this study any possible complex-formation with ferricyanide over the duration of the experiment will be negligible. Further, there is no evidence for this reaction in the membrane-bound system (B. Chance, unpublished work). The experimental conditions are: 15 mg of bovine heart mitochondria/ml containing 5 μ M-cytochrome oxidase (calculated from $\epsilon_{red,ox.605} = 24.0 \text{ mm}^{-1} \cdot \text{cm}^{-1}$; Van Gelder, 1963), 0.2 M-mannitol, 0.75 M-sucrose, 50 mM-sodium phosphate buffer, pH 7.2, 10 mM-succinate, 10 mM-glutamate, 30% (v/v) ethylene glycol, 5 mM-K₃FeCN₆ and 1.2 mM-CO. Two O₂ concentrations (360 μ M and 520 μ M) were used and 2 mm-path-length cuvettes were used throughout for optical studies. The reaction is activated at 173 K by a laser flash from a 0.1 J Rhodamine 6G dye laser that has a wavelength of 585 nm and a pulse width of 1 μ s.

As before (Clare & Chance, 1978), the choice of temperature is governed by the time resolution of the multi-channel spectrophotometer, the turbidity of the mitochondrial suspension resulting in a signal-to-noise ratio that is too low at less than 0.1 s to obtain meaningful data.

Biophysical methods

All the spectrophotometric data at each O₂ concentration were recorded simultaneously from the same sample at the same temperature by using a single laser flash by means of three time-sharing Johnson Foundation multi-channel spectrophotometers

(Chance *et al.*, 1975a), the first two affording wavelengths appropriate to haem kinetics in the region of the α - and γ -bands respectively, and the third appropriate to i.r.-absorbance changes attributable to the kinetics of the copper components of cytochrome oxidase. Further details are as described by Clare & Chance (1978).

Spectroscopic recordings and data digitization

The kinetics were resolved with an amplifier rise time of approx. 0.1 s and recorded on strip charts over a period of approx. 40 min until equilibrium was reached.

Data were digitized by the method developed in Appendix 1 of Clare & Chance (1978). Fig. 1 shows the percentage absorbance change at four wavelength pairs (444–463, 604–630, 608–630 and 830–940 nm) and at two O₂ concentrations (360 and 520 μ M) plotted as a function of logarithmic time. The overall standard error of the data, given by the weighted mean of the standard errors of the individual spectroscopic curves, is $2 \pm 0.26\%$.

Numerical techniques

The numerical techniques of Clare & Chance (1978) were used with a computer program FACSIMILE (Curtis, 1976; Curtis & Kirby, 1977) that employs a modified version of Gear's (1971) method of numerical integration and Powell's (1965, 1972) method of non-linear optimization.

We minimize the residual sum squares (RSQ) given by:

$$\begin{aligned} \text{RSQ} &= \sum_{i=1}^n \sum_{j=1}^m R_{ij}^2 \\ &= \sum_{i=1}^n \sum_{j=1}^m \{ [v_{ij} - (u_{ij}/s_i)] / \sigma_i \}^2 \end{aligned} \quad (1)$$

where j identifies the time point and i the data curve, R_{ij} are the residuals, v_{ij} the observed values, u_{ij} the corresponding calculated values, s_i a scale factor and σ_i the standard error for curve i . At the minimum RSQ is equal to chi-squared (χ^2). From the RSQ we calculate the standard deviation that, unlike the RSQ, is independent of the number of experimental points:

$$\text{s.d.} = \phi \sqrt{\text{RSQ}/(d-p)} \quad (2)$$

where d is the total number of experimental points, p is the number of optimized parameters and ϕ the overall standard error of the data:

$$\phi = \sum \sigma_i r_i / \sum r_i \quad (3)$$

(where r_i is the range of curve i).

The determination of the optimized parameters is given by the s.d._{in} (standard deviation of the

natural logarithm) of the unknown parameter that is obtained from the non-linear co-variance (Clore & Chance, 1978). A parameter whose s.d._{ln} is less than 0.2 is considered to have a well-determined minimum in multidimensional parameter space. For larger values of s.d._{ln}, up to 1 in magnitude, the parameter value is determined to within a factor of order $e \approx 2.72$, and so its order of magnitude is known. Significantly larger values of s.d._{ln} show that the observations are inadequate to determine the parameter. From the s.d._{ln} we calculate the 5-95% confidence limits of the optimized parameters.

A measure of the nature of the distribution of the residuals is given by the correlation index (C_j)

$$C_j = \left(\frac{\sum_I R_j}{\sum_I R_j^2} \right)^{\frac{1}{2}} \quad (4)$$

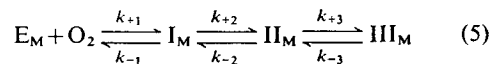
A value of $|C_j|$ significantly greater than 1.0 (the expected root-mean-square value of $|C_j|$ if the residuals were all independent random variables of zero mean and the same variance) indicates that the departures between calculated and observed values are systematic, and statistics such as χ^2 and s.d., the variance-covariance matrix and the s.d._{ln} of the optimized parameters have to be regarded with suspicion. [For the derivation of eqn. (4) see Appendix 3 of Clore & Chance (1978).]

As before (Clore & Chance, 1978), we wish to emphasize that the choice of model in non-linear optimization problems depends not only on obtaining a s.d. within the standard error of the experimental data, but also on obtaining a fit in which the optimized parameters are well determined and the distribution of residuals is random. By providing a rigorous quantitative framework on which to base one's choice of model, this triple requirement greatly decreases the number of models available. In fact, in stiff non-linear problems, it is usually the case that only a single model will satisfy this triple requirement.

Results

Preliminary attempts at non-linear optimization of the coefficients of the differential equations representing a two-intermediate reaction system was found not to fit the data on the basis of s.d. ($\approx 10\%$) and systematic errors in the distribution of residuals. This indicated the presence of other intermediates in the reaction of ferricyanide-pretreated mixed-valence-state membrane-bound cytochrome oxidase with O₂ that had not been identified by low-temperature trapping and wavelength-scanning optical spectroscopy (Chance *et al.*, 1975*b,c*; Chance & Leigh, 1977; Denis & Chance, 1977). A number of other models were then tested involving more intermediates and/or branching pathways, and, as in the case of the

reaction of fully reduced membrane-bound cytochrome oxidase with O₂ (Clore & Chance, 1978), the only model that satisfies the triple requirement of an s.d. within the standard error of the data (i.e. s.d. < 2%), good determination of the optimized parameters and a random distribution of residuals, with no arbitrary constraints, is a three-species sequential mechanism, which is stated as follows:



where E_M is the ferricyanide-pretreated mixed-valence-state cytochrome oxidase complex and intermediate III_M is the product of the reaction. [The subscript M is used to differentiate these intermediates from those in the reaction of fully reduced membrane-bound cytochrome oxidase with O₂ (Clore & Chance, 1978).]

The contribution of each intermediate to each wavelength is represented by a relative absorption coefficient. The crude computed absorbance at the i th wavelength, $W_i(t)$, in units of concentration, is given by:

$$W_i(t) = \sum_l F_l(t) \epsilon'_i(l) \quad (6)$$

where $F_l(t)$ is the concentration of the l th intermediate at time t , and $\epsilon'_i(l)$ is the relative absorption coefficient of the l th intermediate at the i th wavelength (Clore & Chance, 1978).

On the basis of a qualitative interpretation of the data in Fig. 1, the following assignment of intermediates to each wavelength was made. The free mixed-valence-state cytochrome oxidase (E_M) and intermediates I_M , II_M and III_M were assigned to the 444 nm, 604 nm and 608 nm traces:

$$\begin{aligned} W_{444} &= [E_M] \epsilon'_{444}(E_M) + [I_M] \epsilon'_{444}(I_M) \\ &\quad + [II_M] \epsilon'_{444}(II_M) + [III_M] \epsilon'_{444}(III_M) \\ W_{604} &= [E_M] \epsilon'_{604}(E_M) + [I_M] \epsilon'_{604}(I_M) \\ &\quad + [II_M] \epsilon'_{604}(II_M) + [III_M] \epsilon'_{604}(III_M) \\ W_{608} &= [E_M] \epsilon'_{608}(E_M) + [I_M] \epsilon'_{608}(I_M) \\ &\quad + [II_M] \epsilon'_{608}(II_M) + [III_M] \epsilon'_{608}(III_M) \end{aligned} \quad (7)$$

In the case of the 830 nm traces, the absorbance of E_M (which contains e.p.r.-detectable cupric copper, Cu_A^{2+}) is used as the baseline during digitization so that $\epsilon'_{830}(E_M)$ is given *a priori* a value of zero and only intermediates I_M , II_M and III_M are assigned to the 830 nm traces:

$$W_{830} = [I_M] \epsilon'_{830}(I_M) + [II_M] \epsilon'_{830}(II_M) + [III_M] \epsilon'_{830}(III_M) \quad (8)$$

The crude computed absorbance, in units of concentration (given by eqn. 6), is converted into a

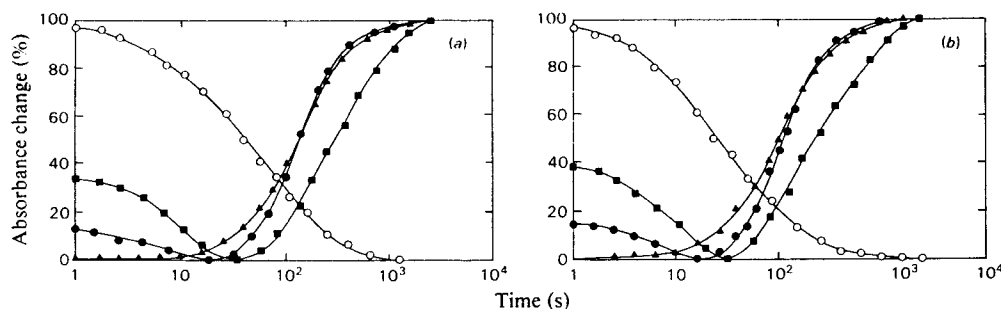


Fig. 1. Observed kinetics of the reaction of ferricyanide-pretreated mixed-valence-state membrane-bound cytochrome oxidase with O_2 at 173 K as measured at four wavelength pairs

Symbols: \circ , 444–463 nm; \bullet , 604–630 nm; \blacksquare , 608–630 nm; \blacktriangle , 830–940 nm. Theoretical curves are shown as solid lines. The experimental conditions are: bovine heart mitochondria, 15 mg/ml containing $5 \mu\text{M}$ -cytochrome oxidase, 30% (v/v) ethylene glycol, 0.2 M-mannitol, 0.75 M-sucrose, 50 mM-sodium phosphate buffer, pH 7.2, 10 mM-succinate, 10 mM-glutamate and 1.2 mM-CO in the presence of $360 \mu\text{M}$ - O_2 (a) and $520 \mu\text{M}$ - O_2 (b).

percentage absorbance change $[N_i(t)\%]$ by means of a scale factor and offset:

$$N_i(t)\% = (W_i(t)S_i - D_i) \times 100 \quad (9)$$

where S_i are the scale factors and D_i the offsets. [Offsets are only required for the 444, 604 and 608 nm traces. In the former trace, characterized by a progressive decrease in absorbance and in the latter two traces, characterized by an initial decrease in absorbance followed by a progressive increase, the experimental points with the minimum absorbance were given a value of zero; however, these points do not correspond to a zero value of W_i and consequently an offset is required. In the case of the 830 nm traces, which are characterized by a progressive increase in absorption, the first experimental point (at $t = 0$ s) was given a value of zero; since W_{830} at $t = 0$ s is zero, no offset is required.]

In the initial optimization, all the following parameters were varied simultaneously.

(a) The rate constants k_{+1} , k_{-1} , k_{+2} , k_{-2} , k_{+3} and k_{-3} .

(b) The relative absorption coefficients of intermediates I_M , II_M and III_M at 444 nm; these were varied relative to $\epsilon'_{444}(E_M)$, which was arbitrarily set to 1.0. The relative absorption coefficients of E_M and intermediates I_M and II_M at 504 and 608 nm; these were varied relative to $\epsilon'_{604}(III_M)$ and $\epsilon'_{608}(III_M)$ respectively, which were arbitrarily set to 1.0. The relative absorption coefficients of intermediates I_M and II_M ; these were varied relative to $\epsilon'_{830}(III_M)$, which was arbitrarily set to 1.0.

(c) The scale factors and offsets for each wavelength at each O_2 concentration (S_{444A} , D_{444A} , S_{444B} , D_{444B} ; S_{604A} , D_{604A} , S_{604B} , D_{604B} ; S_{608A} , D_{608A} , S_{608B} , D_{608B} ; S_{830A} , S_{830B} ; the subscripts A and B refer to the O_2 concentrations of 360 and $520 \mu\text{M}$ respectively.)

All the parameters were well determined except for the rate constant k_{-3} , the offsets at 444 nm (D_{444A} and D_{444B}) and the relative absorption coefficients $\epsilon'_{444}(I_M)$, $\epsilon'_{444}(II_M)$, $\epsilon'_{444}(III_M)$, $\epsilon'_{604}(I_M)$ and $\epsilon'_{608}(I_M)$, whose values were both small and very poorly determined ($s.d._{in} \gg 10$), indicating that the value of these parameters was essentially zero. This indicated that the formation of intermediate III_M is essentially irreversible at this temperature, and that

Table 1. Values of the correlation indices for each curve, the mean absolute correlation index, χ^2 and the overall s.d.

The correlation index (C_i) is a measure of the distribution of residuals. For $|C_i| < 1.0$, the distribution of residuals is random; for $|C_i| \geq 1.0$, the deviations between the calculated and observed values are systematic. Mean absolute correlation index (\bar{C}):

$$0.237 \left(\bar{C} = \frac{1}{k} \sum_{i=1}^k |C_i|, \text{ where } k \text{ is the number of curves} \right)$$

χ^2 : 213 for 217 degrees of freedom (240 observations and 23 parameters). For values of $f > 100$, where f is the number of degrees of freedom, the confidence limits for χ^2 are given by $\frac{1}{2}[(2f-1)^{\pm 1} (1 \pm \xi z_{\alpha/2})]^2$, where $z_{\alpha/2}$ is the value of the standard normal variable at the $\alpha/2$ confidence level and ξ is the fractional error in the estimation of the overall standard error of the data (in this case 0.13). The 99% confidence interval for χ^2 at 217 degrees of freedom is 95.8–386. Overall s.d.: 1.98%. The overall standard error of the data is $2 \pm 0.26\%$ with a 99% confidence interval of 1.33–2.67%.

Wavelength (nm)	Correlation indices	
	360 μM - O_2	520 μM - O_2
444–463	0.779	–0.162
604–630	–0.0911	0.00608
608–630	–0.110	0.174
830–940	–0.287	0.288

Table 2. Optimized values of the parameters together with their s.d._{in} and confidence limits

Parameter number	Parameter	Dimensions	Optimized value	s.d. _{in}	Confidence limits	
					5%	95%
1	k_{+1}	$M^{-1} \cdot s^{-1}$	76.0	0.121	62.2	92.8
2	k_{-1}	s^{-1}	0.0225	0.0927	0.0193	0.0262
3	k_{+2}	s^{-1}	0.0159	0.0756	0.0141	0.0181
4	k_{-2}	s^{-1}	0.000680	0.288	0.000424	0.00109
5	k_{+3}	s^{-1}	0.00168	0.0983	0.00143	0.00198
6	k_{-3}	s^{-1}	$1 \times 10^{-6*}$			
7	$\epsilon'_{444}(I_M) \dagger$		0*			
8	$\epsilon'_{444}(II_M) \dagger$		0*			
9	$\epsilon'_{444}(III_M) \dagger$		0*			
10	$\epsilon'_{604}(E_M) \dagger$		0.422	0.0975	0.360	0.496
11	$\epsilon'_{604}(I_M) \dagger$		0*			
12	$\epsilon'_{604}(II_M) \dagger$		1.00	0.0162	0.974	1.03
13	$\epsilon'_{608}(E_M) \dagger$		0.636	0.0512	0.585	0.692
14	$\epsilon'_{608}(I_M) \dagger$		0*			
15	$\epsilon'_{608}(II_M) \dagger$		0.703	0.0249	0.675	0.733
16	$\epsilon'_{830}(I_M) \dagger$		0*			
17	$\epsilon'_{830}(II_M) \dagger$		0.917	0.0205	0.887	0.948
18	S_{444A}	μM^{-1}	0.200	0.0519	0.184	0.218
19	D_{444A}		0*			
20	S_{444B}	μM^{-1}	0.200	0.0619	0.181	0.221
21	D_{444B}		0*			
22	S_{604A}	μM^{-1}	0.302	0.0433	0.281	0.324
23	D_{604A}		0.504	0.128	0.408	0.622
24	S_{604B}	μM^{-1}	0.287	0.0385	0.269	0.306
25	D_{604B}		0.431	0.128	0.349	0.532
26	S_{608A}	μM^{-1}	0.375	0.0481	0.346	0.406
27	D_{608A}		0.853	0.0989	0.725	1.00
28	S_{608B}	μM^{-1}	0.322	0.0413	0.301	0.345
29	D_{608B}		0.595	0.109	0.497	0.712
30	S_{830A}	μM^{-1}	0.201	0.0139	0.196	0.206
31	S_{830B}	μM^{-1}	0.201	0.00633	0.199	0.203

* k_{-3} , $\epsilon'_{444}(I_M)$, $\epsilon'_{444}(II_M)$, $\epsilon'_{444}(III_M)$, $\epsilon'_{604}(I_M)$, $\epsilon'_{608}(I_M)$, D_{444A} and D_{444B} were constrained at these values on the basis of the initial optimizations in which their values were small and very poorly determined (s.d._{in} \gg 10).

† The relative absorption coefficients at 444, 604, 608 and 830nm are $\epsilon'_{444}(I)$, $\epsilon'_{604}(I)$, $\epsilon'_{608}(I)$ and $\epsilon'_{830}(I)$ respectively, where I is the intermediate referred to. The $\epsilon'_{444}(I)$ were varied relative to $\epsilon'_{444}(E_M)$, which was given a value of 1.0. The $\epsilon'_{604}(I)$, $\epsilon'_{608}(I)$ and $\epsilon'_{830}(I)$ were varied relative to $\epsilon'_{604}(III_M)$, $\epsilon'_{608}(III_M)$ and $\epsilon'_{830}(III_M)$ respectively, which were given a value of 1.0.

the 444nm trace only monitors the kinetics of E_M . In the subsequent optimization these parameters were set to zero except for k_{-3} , which was set to a suitably low value ($1 \times 10^{-6} s^{-1}$). In the resulting solution, all the optimized parameters were well determined. The values of the correlation indices for each curve, the mean absolute correlation index, χ^2 and the overall s.d. of the fit are shown in Table 1; the values of the optimized parameters together with their s.d._{in} and confidence limits are shown in Table 2. The comparison of the experimental and the computed curves is shown in Fig. 1.

Fig. 2 illustrates the kinetics of the individual intermediates and their relationship to the absorbance changes at 444–463, 604–630, 608–630 and 830–940nm. Starting 1s after photolysis of the CO-

inhibited compound the traces begin with the free ferricyanide-pretreated mixed-valence-state cytochrome oxidase at a concentration greater than 95% of its initial value (i.e. $5 \mu M$). Intermediate I_M rises first to a plateau of 35 and 42% of the total enzyme concentration at $360 \mu M$ - and $520 \mu M$ -O₂ respectively. Intermediate I_M is rapidly converted into intermediate II_M , which rises to a later and larger maximum (62 and 65% at $360 \mu M$ - and $520 \mu M$ -O₂ respectively). The reason for the low maxima of intermediates I_M and II_M is because of their rapid conversion into intermediate III_M , which is the final product of the reaction. Table 3 shows the calculated values of the half-times of formation and disappearance of the intermediates at the two O₂ concentrations.

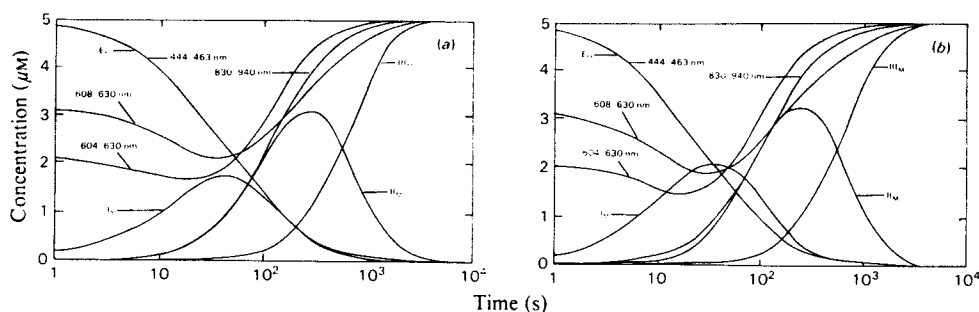


Fig. 2. Computed reaction kinetics of the individual intermediates and their relationship to the theoretical absorbance changes (in units of concentration) at 444–463, 604–630, 608–630 and 830–940 nm in the reaction of ferricyanide-pretreated mixed-valence-state membrane-bound cytochrome oxidase with O_2 at 173 K, as obtained by numerical integration of the differential equations representing a three-intermediate sequential mechanism, by using the values of the rate constants and relative absorption coefficients obtained by optimization

An estimate of the stiffness of the system is given by the ratio of the longest to the shortest time constant: the shortest time constant is $1/(76.0[O_2]) \geq 25.3$ s, and the longest is 10^6 s, giving a ratio of 3.95×10^4 . Initial conditions: $5 \mu M$ -free ferricyanide-pretreated mixed-valence-state cytochrome oxidase (E_M) in the presence of $360 \mu M-O_2$ (a) and $520 \mu M-O_2$ (b).

Table 3. Calculated half-times of formation ($t_{\frac{1}{2} \text{ on}}$) and disappearance ($t_{\frac{1}{2} \text{ off}}$) of the intermediates at $360 \mu M$ - and $520 \mu M-O_2$ at 173 K

	E_M	Inter- mediate I_M	Inter- mediate II_M	Inter- mediate III_M
$t_{\frac{1}{2} \text{ on}}$ (s) at:				
$360 \mu M-O_2$		8.41	70.8	596
$520 \mu M-O_2$		7.08	63.1	562
$t_{\frac{1}{2} \text{ off}}$ (s) at:				
$360 \mu M-O_2$	37.6	168	841	
$520 \mu M-O_2$	23.7	133	794	

Discussion

General assumptions in the assignment of valence states of the four metal centres to the intermediates

In the following sections we attempt to assign valence states to the four metal centres of cytochrome oxidase in each of the intermediates. In doing so we recognize that it may be an oversimplification to assume that electrons are localized on particular metal centres rather than being distributed in some statistical manner among them.

Only two species A_2 and C have been trapped at low temperatures in the reaction of ferricyanide-pretreated mixed-valence-state membrane-bound cytochrome oxidase with O_2 and characterized by optical wavelength scanning and e.p.r. spectroscopy (Chance *et al.*, 1975b,c; Chance & Leigh, 1977; Denis & Chance, 1977). In the discussion that follows, we make the following general assumptions about the relationship of these two species with the three kinetically identified intermediates of this study.

(1) Compound A_2 is equivalent to intermediate II_M . This seems reasonable, since compound A_2 was trapped at 177 K 10 s after flash photolysis (Chance *et al.*, 1975c), and Fig. 3 shows that at 173 K the concentration of intermediates II_M and III_M is negligible relative to that of intermediate I_M up to about 30 s after flash photolysis.

(2) Compound C is equivalent to intermediate III_M . This seems reasonable, since compound C is the stable end product of the reaction in the range 163–265 K (Chance & Leigh, 1977).

Therefore in the following discussion the first and third intermediates in the reaction will be referred to as intermediates I_M and III_M rather than compounds A_2 and C.

In addition, we make the following assumptions about the nature of the contributions to the 444, 604, 608 and 830 nm traces.

(1) Only free haem a_3^{2+} and free haem a^{2+} (i.e. not interacting with O_2) contribute to the absorbance at 444 nm (Lemberg, 1969). Thus haem a_3^{2+} and haem a^{2+} directly interacting with O_2 , haem a_3^{3+} and haem a^{3+} , and higher valence states of haem iron [Fe(IV) and greater], do not contribute to the 444 nm traces. The latter assumption is by analogy with compound I of horseradish peroxidase in which haem iron is in the Fe(IV) state (Dolphin *et al.*, 1971).

(2) Haem a_3^{3+} and haem a^{3+} do not contribute to the absorbance of the 600–610 nm band in the α -region of the cytochrome oxidase spectrum (Wikström *et al.*, 1976). Thus in the presence of both haem a_3^{3+} and haem a^{3+} the relative absorption coefficients at both 604 and 608 nm are zero.

(3) The relative contribution of haem a_3^{2+} and haem a^{2+} at 604nm and 608nm may be affected by haem-haem (Wikström *et al.*, 1976) and haem-copper (Palmer *et al.*, 1976) interactions (by which is meant all mechanisms by which any modification in one of the metal components of cytochrome oxidase may affect the properties of the others), and by interactions with ligands (Wilson & Leigh, 1974).

(4) Copper is the major, if not only, contributor to the 830nm traces (Aasa *et al.*, 1976; Wever *et al.*, 1977).

In the discussion that follows, we attempt to assign particular valence states to the haem and copper moieties in each intermediate on the basis of the optimized values of the relative absorption coefficients of the intermediates at each wavelength obtained from the present paper, and the optical wavelength scanning and e.p.r. data on intermediates I_M and III_M (Chance *et al.*, 1975*b,c*; Chance & Leigh, 1977; Denis & Chance, 1977). The reaction sequence, together with the optimized values of the relative absorption coefficients, rate constants and equilibrium constants at 173 K, and the proposed valence states of the four metal centres in each intermediate, is summarized in Table 4.

Assignment of valence states of the four metal centres to the intermediates

The 830nm traces are best fitted by nearly equal contributions from intermediates II_M and III_M, and no contribution from E_M and intermediate I_M (see Tables 2 and 4). Since the absorbance of E_M (in which Cu_A is in the cupric state) is used as the baseline during digitization so that $\epsilon'_{830}(E_M)$ is given *a priori*

a value of zero, and since the intensity of the e.p.r. signal due to cupric copper at $g = 2$ is approximately the same in E_M and intermediates I_M and III_M (Chance & Leigh, 1977), we deduce, on the basis of our initial assumptions, that Cu_A remains in the cupric state in intermediates I_M and III_M, and that Cu_B is in the cuprous state in intermediate I_M and in the cupric state in intermediate III_M. The finding that $\epsilon'_{830}(II_M)$ is nearly equal to $\epsilon'_{830}(III_M)$ strongly suggests that the configuration of the copper atoms in intermediate II_M is the same as that in intermediate III_M, namely Cu_A²⁺Cu_B²⁺. It should be noted, however, that the difference between $\epsilon'_{830}(III_M)$ and $\epsilon'_{830}(II_M)$, though small, is significant [$\epsilon'_{830}(III_M) - \epsilon'_{830}(II_M) = 0.083 \pm 0.019$; also see Table 2], and we attribute this to copper-copper and/or copper-haem interactions.

The observation that the intensity of the e.p.r. signal due to low-spin ferric haem at $g = 3.05$ is approximately the same in E_M and intermediates I_M and III_M strongly suggests that haem *a* is in the ferric state in intermediates I_M and III_M. Further evidence that haem *a* remains in the ferric state in intermediate III_M is afforded by the formation of intermediate III_M at temperatures as high as 265 K (Chance & Leigh, 1977), where ferricyanide is the active oxidant of haem *a* and its reduction to any significant extent would seem unlikely.

Tables 2 and 4 show that, within the errors specified, for the 444nm traces:

$$\begin{aligned} \epsilon'_{444}(E_M) &= 1.0 \\ \epsilon'_{444}(I_M) &= \epsilon'_{444}(II_M) = \epsilon'_{444}(III_M) = 0 \end{aligned} \quad (10)$$

Table 4. Proposed chemical identity of the intermediates and the reaction sequence at 173 K, with the optimized values of the rate constants and relative absorption coefficients, and the calculated value of the equilibrium constants together with their s.d._{in} and confidence limits

The s.d._{in} and 5–95% confidence limits of the equilibrium constants are calculated from the s.d._{in} of the individual rate constants (given in Table 2) and the correlation coefficient (*r*) relating the forward and backward rate constants by using the formula $(\psi_i^2 - 2r\psi_i\psi_j + \psi_j^2)^{1/2}$, where ψ_i and ψ_j are the s.d._{in} of the forward and backward rate constants.

Reaction sequence and rate constants at 173 K	O ₂ + E _M	I _M	II _M	III _M
	$\xrightarrow[k_{-1}]{76.0M^{-1}s^{-1}}$	$\xrightleftharpoons[k_{-2}]{0.0159s^{-1}}$	$\xrightleftharpoons[k_{-3}]{0.00168s^{-1}}$	
		$\xleftarrow[0.000680s^{-1}]{} I_M$	$\xleftarrow[1 \times 10^{-6}s^{-1}]{} II_M$	
Equilibrium constants (k_{+i}/k_{-i})		3380 M ⁻¹	23.4	1680
correlation coefficient (<i>r</i>)		0.624	0.106	
s.d. _{in} *		0.0961	0.290	
5–95% confidence limits		2890–3960 M ⁻¹	14.5–37.7	
Relative absorption coefficients at:				
444–463 nm [$\epsilon'_{444}(I)$]	1.0 (100%)	0 (0%)	0 (0%)	0 (0%)
604–630 nm [$\epsilon'_{604}(I)$]	0.422 (17.4%)	0 (0%)	1.00 (41.3%)	1.0 (41.3%)
608–630 nm [$\epsilon'_{608}(I)$]	0.636 (27.2%)	0 (0%)	0.703 (30.0%)	1.0 (42.8%)
830–940 nm [$\epsilon'_{830}(I)$]	0 (0%)	0 (0%)	0.917 (47.8%)	1.0 (52.2%)
Proposed chemical identity of the intermediates	$a_3^{2+}Cu_B^+$ $a^3+Cu_A^{2+}$	$a_3^{3+}Cu_B^+$ $a^3+Cu_A^{2+} \cdot O_2^-$	$a_3^?Cu_B^{2+} \cdot O_2^?$	$a_3^?Cu_B^{2+}$ $a^3+Cu_A^{2+} \cdot O_2^?$

for the 604 nm traces:

$$\begin{aligned}\epsilon'_{604}(\text{III}_M) &= \epsilon'_{604}(\text{II}_M) \\ \epsilon'_{604}(\text{II}_M) &> \epsilon'_{604}(\text{E}_M) \\ \epsilon'_{604}(\text{I}_M) &= 0\end{aligned}\quad (11)$$

and for the 608 nm traces:

$$\begin{aligned}\epsilon'_{608}(\text{III}_M) &> \epsilon'_{608}(\text{II}_M) > \epsilon'_{608}(\text{E}_M) \\ \epsilon'_{608}(\text{I}_M) &= 0\end{aligned}\quad (12)$$

Since the relative absorption coefficients of intermediate I_M at both 604 and 608 nm are zero, we deduce, on the basis of our initial assumptions, that both haem a_3 and haem a are in the ferric state in intermediate I_M .

On the basis of the evidence presented so far, a basic scheme can be constructed (see Table 4). The valence states of haem a_3 and haem a in intermediate II_M , the valence state of haem a_3 in intermediate III_M and the number of electrons donated to O_2 in intermediates II_M and III_M are not specified. The first step involves a one-electron reduction of O_2 resulting in the production of a superoxide ion (O_2^-) and the oxidation of haem a_3 to the ferric state ($a_3^{3+} \cdot \text{O}_2^-$), rather than simple ligand binding without electron transfer to form an oxy compound of the ferrous haem ($a_3^{2+} \cdot \text{O}_2$) as suggested by Chance *et al.* (1975*b,c*). These authors have argued against the presence of O_2^- in intermediate I_M on the basis that they did not observe a high-spin haem e.p.r. signal at $g = 6$ (Chance *et al.*, 1978) attributable to high-spin haem a_3^{3+} in the absence of anti-ferromagnetic coupling of haem a_3^{3+} to Cu_B^{2+} (Palmer *et al.*, 1976) and broadening of the e.p.r. signals at $g = 3.05$ and $g = 2$ attributable to the presence of the paramagnetic O_2^- (Chance *et al.*, 1975*b,c*). However, just as one of the unpaired electrons on high-spin haem a_3^{3+} is spin-coupled with the unpaired electron on Cu_B^{2+} resulting in the formation of an anti-ferromagnetically spin-coupled haem-copper dimer that is not visible by e.p.r. (Palmer *et al.*, 1976; Thomson *et al.*, 1976, 1977; Falk *et al.*, 1977), it seems likely that one of the unpaired electrons on high-spin haem a_3^{3+} could also undergo spin-coupling with the unpaired electron O_2^- resulting in the formation of an exchange-coupled complex of even spin ($S = 2$ or 3), which would be difficult or impossible to observe by e.p.r.

Any assignment of valence states of haem a_3 and haem a in intermediate II_M , and haem a_3 in intermediate III_M must account for the following observations.

(a) The absence of any contribution from intermediates II_M and III_M to the 444 nm traces.

(b) The intense absorption band at 606–609 nm associated with intermediate III_M (Chance *et al.*, 1975*b,c*; Chance & Leigh, 1977; Denis & Chance, 1977).

(c) The finding that there is a significant increase in the relative absorption coefficient of intermediate III_M with respect to that of intermediate II_M at 608 nm ($\epsilon'_{608}(\text{III}_M) - \epsilon'_{608}(\text{II}_M) = 0.297 \pm 0.017$; also see Table 2), but that the relative absorption coefficients of intermediates II_M and III_M at 604 nm are equal (i.e. this suggests the presence of a 606–609 nm band in intermediate II_M , which is blue-shifted with respect to that of intermediate III_M).

(d) The 655 nm band, which, on the basis of e.p.r. (Beinert *et al.*, 1976) and m.c.d. (Palmer *et al.*, 1976) studies, is thought to arise as a consequence of anti-ferromagnetic coupling between high-spin haem a_3^{3+} and Cu_B^{2+} , is not formed during the course of the reaction (Chance & Leigh, 1977; Denis & Chance, 1977).

(e) The stability of intermediate III_M at temperatures up to as high as 265 K (Chance & Leigh, 1977).

If we exclude all states where haem a_3^{3+} and haem a^{3+} coexist on the basis that the relative absorption coefficients of intermediates II_M and III_M are not zero at 604 and 608 nm, and assume that the maximum number of electrons that can be donated to O_2 is four, and that reduced O_2 species are not reoxidized, we are left with three alternative schemes to account for the above observations (see Fig. 3).

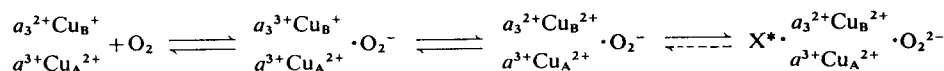
In Fig. 3 (Scheme 1), the formation of intermediate II_M involves an internal oxidation–reduction resulting in the oxidation of Cu_B to the cupric state and the reduction of haem a to the ferrous state. This is followed by a further internal oxidation–reduction resulting in the re-oxidation of haem a to the ferric state and the reduction of haem a_3 to the ferrous state in intermediate III_M . Although the intense absorption at 606–609 nm could be accounted for by interaction between haem a^{2+} , Cu_B^{2+} and O_2^- in intermediate II_M , and between haem a_3^{2+} , Cu_B^{2+} and O_2^- in intermediate III_M resulting in the generation of a charge transfer band, this scheme would have difficulty in accounting for both the absence of a 655 nm band and the absence of any contribution from intermediate II_M to the 444 nm traces. The unpaired electron on O_2^- could undergo spin-coupling with one of the unpaired electrons on high-spin haem a_3^{3+} and thereby prevent anti-ferromagnetic coupling between high-spin haem a_3^{3+} and Cu_B^{2+} (which would account for the absence of the 655 nm band), but it seems unlikely that O_2^- could interact at the same time with haem a^{2+} to account for the absence of any contribution of intermediate II_M to the 444 nm traces.

In Fig. 3 (Scheme 2), the formation of intermediate II_M involves an internal oxidation–reduction resulting in the oxidation of Cu_B to the cupric state and the reduction of haem a_3 to the ferrous state. The formation of intermediate III_M is then associated with a one-electron reduction of O_2^- to the O_2^{2-} state and the production of a free cation radical X^* .

Scheme 1



Scheme 2



Scheme 3

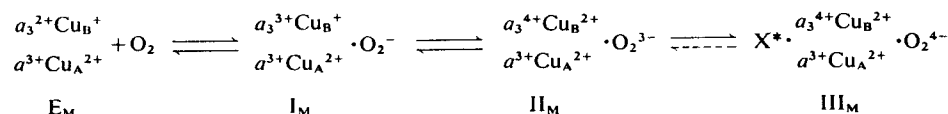


Fig. 3. Three schemes for the reaction of ferricyanide-pretreated mixed-valence-state membrane-bound cytochrome oxidase with O₂

Since it is not known at present at what stage cleavage of the O–O bond occurs, whether cleavage is homolytic or heterolytic, and whether protonation takes place at this low temperature, the reduced-O₂ species are represented as O₂^{x-}, where x indicates the number of electrons donated to O₂.

In Fig. 3 (Scheme 3), the formation of intermediate II_M involves a two-electron reduction of O₂⁻ to the O₂³⁻ state resulting in the oxidation of haem a₃ and Cu_B to the quadrivalent [Fe(IV)] and cupric states respectively. The formation of intermediate III_M is then associated with a one-electron reduction of O₂³⁻ to the O₂⁴⁻ state and the production of a free cation radical X*.

In Schemes 2 and 3 of Fig. 3, the free cation radical X* in intermediate III_M is envisaged as a porphyrin π-cation radical as in compound I of horseradish peroxidase (Dolphin *et al.*, 1971) rather than a protein-cation radical as in compound ES of cytochrome *c* peroxidase (Yonetani, 1976) on the basis that the free-radical e.p.r. signal at *g* = 2 in compound ES has not been observed in intermediate III_M (Chance *et al.*, 1975*b*). In the case of a porphyrin π-cation radical, an electron localized on the porphyrin will couple through exchange interactions with spin-localized on the haem iron (Dolphin *et al.*, 1971), resulting in broadening of the e.p.r. signal beyond the limit of detection. The known stability of a number of porphyrin π-cation radicals (Dolphin *et al.*, 1971) would then explain the observed stability of intermediate III_M at temperatures as high as 265 K.

Both Schemes 2 and 3 of Fig. 3 account for the absence of a 655 nm band since neither scheme allows for anti-ferromagnetic coupling between high-spin haem a₃³⁺ and Cu_B²⁺. The absence of any contribution of intermediates II_M and III_M to the 444 nm traces is also accounted for since in Scheme 2 haem a₃²⁺ can interact directly with O₂⁻ and O₂²⁻ in intermediates II_M and III_M respectively, and in

Scheme 3 haem a₃ and haem *a* are in the quadrivalent and ferric states respectively in intermediates II_M and III_M. In the case of Scheme 2, the intense absorption band at 606–609 nm is attributed to a charge-transfer band arising from interaction between haem a₃²⁺, Cu_B²⁺ and O₂⁻ in intermediate II_M, and between haem a₃²⁺, Cu_B²⁺, X* and O₂²⁻ in intermediate III_M. In the case of Scheme 3, the 606–609 nm band is attributed to the presence of quadrivalent iron in intermediates II_M and III_M by analogy with the absorption bands in the 600–700 nm region attributed to quadrivalent iron in compounds I and II of horseradish peroxidase (Dolphin *et al.*, 1971) and compound ES of cytochrome *c* peroxidase (Yonetani, 1976).

On the basis of the evidence and arguments presented, Scheme 1 of Fig. 3 seems highly unlikely. Schemes 2 and 3 of Fig. 3, however, can both account equally well for the present data, and will require Mössbauer spectroscopy and low-temperature magnetic-susceptibility measurements to discriminate between them.

We thank Dr. B. Chance and Mr. A. R. Curtis for stimulating discussions, criticism and continual encouragement. We thank the Johnson Research Foundation for experimental facilities and the University College London Computer Centre for computing facilities. G. M. C. acknowledges a Carlo Campolin Scholarship.

References

- Aasa, R., Albracht, S. P. J., Falk, K.-E., Lanne, B. & Vanngård, T. (1976) *Biochim. Biophys. Acta* **422**, 260–272

- Beinert, H., Hansen, R. E. & Hartzell, C. R. (1976) *Biochim. Biophys. Acta* **423**, 339-355
- Caughey, W. S., Wallace, W. J., Volpe, J. A. & Yoshikawa, S. (1976) *Enzymes 3rd Ed.* **13**, 299-344
- Chance, B., & Leigh, J. S. (1977) *Proc. Natl. Acad. Sci. U.S.A.* **74**, 4777-4780
- Chance, B., Legallais, V., Sorge, J. & Graham, N. (1975a) *Anal. Biochem.* **66**, 498-514
- Chance, B., Saronio, C. & Leigh, J. S. (1975b) *Proc. Natl. Acad. Sci. U.S.A.* **72**, 1635-1640
- Chance, B., Saronio, C. & Leigh, J. S. (1975c) *J. Biol. Chem.* **250**, 9226-9237
- Chance, B., Saronio, C., Leigh, J. S., Ingledew, W. J. & King, T. E. (1978) *Biochem. J.* **171**, 787-798
- Clore, G. M. & Chance, E. M. (1978) *Biochem. J.* **173**, 799-810
- Curtis, A. R. (1976) *A.E.R.E. Rep. No. C.S.S. 26*, A.E.R.E., Harwell
- Curtis, A. R. & Kirby, C. R. (1977) *A.E.R.E. Rep. No. C.S.S. 46*, A.E.R.E., Harwell
- Denis, M. & Chance, B. (1977) *Abstr. FEBS Meet. 11th* abstr. no. A-4-11-716
- Dolphin, D., Forman, A., Borg, D. C., Fajer, J. & Felton, R. H. (1971) *Proc. Natl. Acad. Sci. U.S.A.* **68**, 614-618
- Falk, K.-E., Vanngård, T. & Angström, J. (1977) *FEBS Lett.* **75**, 23-27
- Gear, C. W. (1971) *Commun. ACM* **14**, 176-179
- Lanne, B., Malmström, B. & Vanngård, T. (1977) *FEBS Lett.* **77**, 146-150
- Lemberg, M. R. (1969) *Physiol. Rev.* **49**, 48-121
- Lindsay, J. G. & Wilson, D. F. (1974) *FEBS Lett.* **48**, 45-49
- Lindsay, J. G., Owen, C. S. & Wilson, D. F. (1975) *Arch. Biochem. Biophys.* **169**, 492-505
- Mackay, L. N., Kuwana, T. & Hartzell, C. R. (1973) *FEBS Lett.* **36**, 326-329
- Muijsers, A. O., Tiesjema, R. H., Henderson, R. W. & Van Gelder, B. F. (1972) *Biochim. Biophys. Acta* **267**, 216-221
- Palmer, G., Babcock, G. T. & Vickery, L. E. (1976) *Proc. Natl. Acad. Sci. U.S.A.* **73**, 2206-2210
- Powell, M. J. D. (1965) *Comput. J.* **7**, 303-307
- Powell, M. J. D. (1972) *A.E.R.E. Rep. No. T.P. 402*, A.E.R.E., Harwell
- Thomson, A. J., Brittain, T., Greenwood, C. & Springall, J. P. (1976) *FEBS Lett.* **67**, 94-98
- Thomson, A. J., Brittain, T., Greenwood, C. & Springall, J. P. (1977) *Biochem. J.* **165**, 327-336
- Van Gelder, B. F. (1963) *Biochim. Biophys. Acta* **73**, 663-665
- Wever, R., Van Drooge, J. H., Muijsers, A. O., Bakker, E. P. & Van Gelder, B. F. (1977) *Eur. J. Biochem.* **73**, 149-154
- Wikström, M. K. F., Harmon, H. J., Ingledew, W. J. & Chance, B. (1976) *FEBS Lett.* **65**, 259-277
- Wilson, D. F. & Leigh, J. S. (1974) *Ann. N.Y. Acad. Sci.* **227**, 630-635
- Wilson, D. F., Erecinska, M. & Lindsay, J. G. (1975) in *Electron Transfer Chains and Oxidative Phosphorylation* (Quagliariello, E., Papa, S., Palmieri, F., Slater, E. C. & Siliprandi, N., eds.), pp. 69-74, North-Holland, Amsterdam
- Yonetani, T. (1976) *Enzymes 3rd Ed.* **13**, 345-361, Academic Press, New York